ROCKETS' STABILIZATION CONTROL SYSTEMS USING DIFFERENTIATOR OR INTEGRATOR GYROSCOPES

Mihai LUNGU

Avionics Department, University of Craiova, Faculty of Electrotechnics,
Decebal Blv., No.107, Craiova, Dolj, ROMANIA
Lma1312@yahoo.com, mlungu@elth.ucv.ro

***Abstract* – The paper presents the comparison between two angular stabilization systems of the rockets in vertical plane using a differentiator or an integrator gyroscope, an accelerometer and a correction subsystem. One has determined the transfer functions (in closed loop or in open loop) of the system in the complex variable or in discrete variable. All the eigenvalues of the system are placed in the left complex semi-plane (the proof of system's stability). For both systems one obtains, using a Matlab/Simulink program, the indicial functions in the complex plane and in discrete plane, responses to impulse input in the complex and discrete planes. The identification of the systems is made using neural networks' method. One obtained the indicial responses of the control system and of the neural network after the training process and the dependence between the training error and the training epochs' number.**

***Keywords*:** *rocket, differentiator gyroscope, integrator gyroscope.*

1. DYNAMICS OF THE ROCKETS' MOVEMENT

The stabilization systems for the anti-aircraft rockets, air-to-air rockets and ground-air rockets fulfill the functions of control over the load. Since most of these oscillations damping is weak $(\xi \le 0{,}1)$, it is difficult to control the overload. The more the speed and flight altitude increases, the more difficult this mission is. Thus, the stabilization systems must correct the dynamic characteristics of the rockets. One also requires that the stabilization systems reduce the influence of external disturbances and internal noise. Thus, control's bandwidth and disturbance signals are chosen according to technical quality indicators [1].
Next, one studies the stabilization systems' dynamics of rockets with cross empennage. Mathematical model of rocket's motion in the vertical plane is given by equations' system (1), the coefficients being those of form (2).

$$\begin{cases} \dot{\theta} = d_1\alpha + d_5\delta, \\ \dot{\omega}_z = d_3\alpha - d_2\delta - d_4\omega_z, \\ \dot{\theta} = \omega_z, \alpha = \theta - \vartheta, \end{cases} \tag{1}$$

where θ is the pitch angle of the rocket, ω_z – the pitch angular velocity, α – the incidence angle of the rocket, δ – the rocket's command, ϑ – the slope of the trajectory; the other terms are coefficients with formula [2]

$$d_1 = \frac{\rho\frac{V^2}{2}Sc_y^{\alpha} + F_T}{mV} = \frac{1}{T_V}, d_2 = \frac{\rho\frac{V^2}{2}SlC_z^{\delta}}{J_z},$$
$$d_3 = \frac{\rho\frac{V^2}{2}SlC_z^{\alpha}}{J_z}, d_4 = \frac{\rho\frac{V^2}{2}Sl^2C_z^{\omega}}{J_z}, d_5 = \frac{\rho\frac{V^2}{2}Sc_y^{\delta}}{mV}. \tag{2}$$

To obtain the step and impulse responses and the identification of the system, one uses the following coefficients

$$T_1 = \frac{1}{d_1} = T_V, T_2 = \frac{1}{\sqrt{d_1d_4 - d_3}}, \xi = \frac{1}{2}\frac{d_1 + d_4}{\sqrt{d_1d_4 - d_3}},$$
$$k_{\theta} = \frac{d_1d_2}{d_1d_4 - d_3}, k_{\alpha} = \frac{d_2}{d_1d_4 - d_3}, k_W = k_{\theta}V. \tag{3}$$

In the case of vertical flight of the rockets, the above equations set suffers little modifications

$$T_1 = \frac{1}{d_1} = T_V, T_2 = \frac{1}{\sqrt{d_1d_4 + d_3}}, \xi = \frac{1}{2}\frac{d_1 + d_4}{\sqrt{d_1d_4 + d_3}},$$
$$k_{\theta} = \frac{d_1d_2}{d_1d_4 + d_3}, k_{\alpha} = \frac{d_2}{d_1d_4 + d_3}, k_W = k_{\theta}V. \tag{4}$$

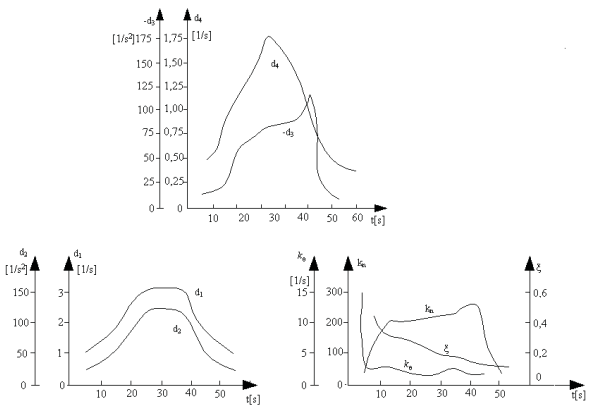

Figure 1: Time variation curves of the coefficients from rockets' dynamics equations

For each rocket's type one must obtain the variation

in time of coefficients d_i, $i = \overline{1,5}$. In figure 1 the time variation curves of these coefficients for an ERLIKON rocket are presented. The values of these coefficients for second 10 of the flight are

$$\begin{aligned} d_1 &= 1.125\left[1/s\right]; d_2 = 25\left[1/s^2\right]; \\ d_3 &= 14.285\left[1/s^2\right]; d_4 = 0.535\left[1/s\right]. \end{aligned} \quad (5)$$

The coefficients d_i characterize the stability of the system and the stability reserves; if $d_5 = 0$, then $n_v^\alpha = d_1$. The maneuverability of the system may be expressed on a graded scale which permits the choose of optimal maneuverability [1].

The maneuverability of the system depends on an indicator which expresses the dependence of the ratio T_2 / T_1 or of the product $n_v^\alpha T_2$ of the damp coefficient ξ. For the stability's improvement and maneuverability's increase one uses a negative feedback after the rockets' overload n_v; it leads to the increase of the damp coefficient.

2. ANGULAR STABILIZATION SYSTEM WITH DIFFERENTIATOR GYROSCOPE, ACCELEROMETER AND CORRECTION SUBSYSTEM

Stabilization system that uses differentiator gyroscope, although has superior dynamic performances, doesn't assure their constant in different flight regimes. That's why, this system is recommended only for the stabilization of the rockets' angular position. The mono-loop stabilization systems have some disadvantages which prevent their use for the overload's control. Much better are the bi-loop stabilization systems.

The block diagram of the rockets' angular stabilization system with differentiator gyroscope, accelerometer and correction subsystem is presented in figure 2 [1]. The input variable is the rocket's command u_v, while the output of the system is the rocket's overload n_v. On the direct way of the system one has introduced an integrator gyroscope and on the feedback of the exterior contour – an acceleration transducer (accelerometer), a correction network with the transfer function

$$H_c(\mathrm{s}) = \frac{T_4'}{T_3'}\frac{T_3'\mathrm{s}+1}{T_4'\mathrm{s}+1} \quad (6)$$

and an amplifier with k_k amplification factor for the compensation of the voltage's failure at the output of the correction network (subsystem). The transfer function of the interior loop is calculated as follows

$$H_i(\mathrm{s}) = \frac{k_v \cdot \frac{k_s}{T_s\mathrm{s}+1} \cdot \frac{k_n}{T_2^2\mathrm{s}^2 + 2\xi T_2\mathrm{s}+1}}{1 + \frac{57.3\mathrm{g}}{\mathrm{V}}(T_1\mathrm{s}+1) \cdot \frac{T_4}{T_3} \cdot \frac{T_3\mathrm{s}+1}{T_4\mathrm{s}+1} \cdot k_d \cdot k_v \cdot \frac{k_s}{T_s\mathrm{s}+1} \cdot \frac{k_n}{T_2^2\mathrm{s}^2 + 2\xi T_2\mathrm{s}+1}}. \quad (7)$$

The closed loop transfer function is obtained with equation

$$H_{u_v}^{n_v}(\mathrm{s}) = \frac{n_v(\mathrm{s})}{u_v(\mathrm{s})} = k_u \cdot \frac{H_i(\mathrm{s})}{1 + k_k \cdot \frac{T_4'}{T_3'} \cdot \frac{T_3'\mathrm{s}+1}{T_4'\mathrm{s}+1} \cdot k_a \cdot H_i(\mathrm{s})}. \quad (8)$$

In equations (7) and (8) the values of the constants are

$$\begin{aligned} &T_1 = 1/d_1; T_2 = \frac{1}{\sqrt{d_1 d_4 + d_3}}; T_3 = 0.3\,\mathrm{sec}; T_4 = 0.03\,\mathrm{sec}; \\ &T_s = 0.1\,\mathrm{sec}; T_i = 1\,\mathrm{sec}; V = 1800\,\mathrm{Km/h}; g = 9.81\,\mathrm{m}/s^2; \\ &\xi = 0.05; k_v = 0.5; k_n = 14.4\,\mathrm{deg/V}; k_s = 1; \\ &k_i = 0.4\,\mathrm{V/deg}; k_k = 1.8; k_u = 0.75; k_a = 0.4\,\mathrm{V/deg}; \\ &T_3' = 0.056\,\mathrm{sec}; T_4' = 0.001\,\mathrm{sec}. \end{aligned} \quad (9)$$

After calculus, the transfer function in closed loop becomes

$$H_0(\mathrm{s}) = \frac{n_v(\mathrm{s})}{u_v(\mathrm{s})} = \frac{B_2\mathrm{s}^2 + B_1\mathrm{s} + B_0}{A_5\mathrm{s}^5 + A_4\mathrm{s}^4 + A_3\mathrm{s}^3 + A_2\mathrm{s}^2 + A_1\mathrm{s} + A_0}; \quad (10)$$

the transfer function in open loop is calculated in rapport with the one presented above. The coefficients that appear in the numerator and dominator of the transfer function (10) are

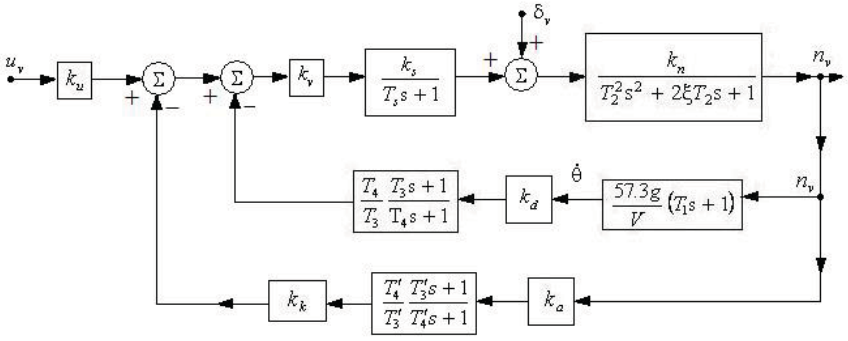

Figure 2: The block diagram of the rockets' angular stabilization system with differentiator gyroscope, accelerometer and correction subsystem

$$
\begin{aligned}
&B_2 = k_u k_v k_s k_n V T_3 T_3' T_4 T_4' \,;\; B_1 = k_u k_v k_s k_n V T_3 T_3' \cdot (T_4 + T_4') \,;\\
&B_0 = k_u k_v k_s k_n V T_3 T_3' \,;\\
&A_5 = T_3 T_3' V T_s T_4 T_4' T_s T_2^2 \,;\\
&A_4 = T_3 T_3' V \left(T_2^2 T_4 T_4' + 2\xi T_2 T_s T_4 T_4' V\right) + T_3 T_3' V \left[T_s T_2^2 (T_4 + T_4')\right];\\
&A_3 = T_3 T_3' V \left[2\xi T_2 T_4 T_4' + T_s T_4 T_4' + T_2^2 (T_4 + T_4')\right] +\\
&+ T_3 T_3' V \left[T_s T_2^2 + 2\xi T_s T_2 (T_4 + T_4')\right] + 57.3 g k_v k_s k_n k_d T_4 T_3' (T_1 T_3 + T_4');\\
&A_2 = T_3 T_3' V \left[T_4 T_4' + 2\xi T_2 (T_4 + T_4') + T_s (T_4 + T_4') + T_2^2 + 2\xi T_s T_2\right] +\\
&+ 57.3 g k_v k_s k_n k_d T_4 T_3' (T_1 T_4' + T_1 T_3 + T_3 T_4') + k_a k_k k_v k_s k_n T_3 T_4' V T_3' T_4 \,;\\
&A_1 = T_3 T_3' V (T_4 + T_4' + 2\xi T_2 + T_s) + + k_a k_k k_v k_s k_n T_3 T_4' V (T_3' + T_4') +\\
&+ 57.3 g k_v k_s k_n k_d T_4 T_3' (T_4' + T_1 + T_3);\\
&A_0 = T_3 T_3' V + 57.3 g k_v k_s k_n k_d T_4 T_3' + k_a k_k k_v k_s k_n T_3 T_4' V \,.
\end{aligned}
\tag{11}
$$

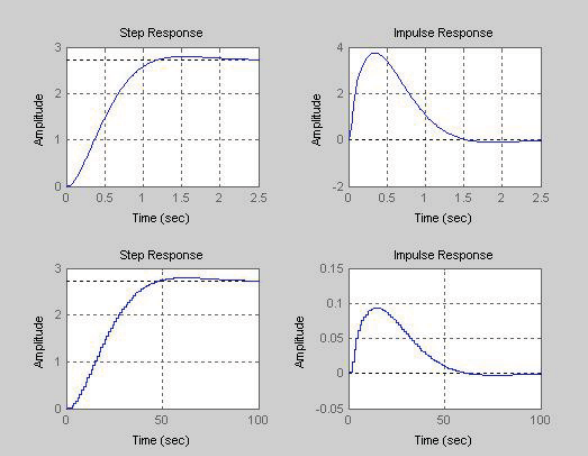

Figure 3: The indicial functions and responses to impulse input in the complex and discrete planes for the system from figure 2

For the above system one obtains, using a Matlab program and a Simulink model, the indicial functions in the complex plane and in discrete plane, responses to impulse input in the complex and discrete planes and time variations of the rocket's overload and of the pitch angular velocity. For the system from figure 2, the indicial functions and responses to impulse input in the complex and discrete planes are presented in figure 3 (the first two graphics correspond to the complex plane, while the last two correspond to the discrete plane).

The program calculates the matrices that describe the state equations of the system in the complex or discrete plane, the poles of the system, the zeros, the transfer functions in complex description or in discrete description, the stability margins and so on.

For the stabilization system, one plots the time variation of the system's output – rocket's overload (n_v) and time variation of the pitch angular velocity $(\dot{\theta})$ - figure 4.

From these graphic characteristics and from the analysis of the system's eigenvalues (poles) one notices that the system is a stable one with very good dynamic properties.

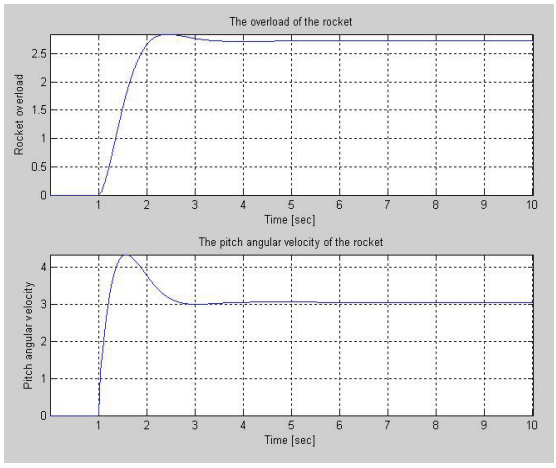

Figure 4: Time variation of the rochet's overload and time variation of the rocket's angular velocity

3. ANGULAR STABILIZATION SYSTEM WITH INTEGRATOR GYROSCOPE, ACCELEROMETER AND CORRECTION SUBSYSTEM

The block diagram of the rockets' angular stabilization system with integrator gyroscope, accelerometer and correction subsystem is presented in figure 5 [1]. The input and the output variables are the same with the ones from the previous case.

On the direct way of the system one has introduced an integrator gyroscope and on the feedback of the exterior contour – an acceleration transducer (accelerometer), a correction network with the transfer function

$$H_c(\mathrm{s}) = \frac{T_4}{T_3}\,\frac{T_3\mathrm{s}+1}{T_4\mathrm{s}+1} \tag{12}$$

and an amplifier with k_k amplification factor for the compensation of the voltage's failure at the output of the correction network (subsystem). The transfer function of the interior loop is calculated as follows

$$H_i(\mathrm{s}) = \frac{\dfrac{k_i(T_i\mathrm{s}+1)}{\mathrm{s}} \cdot \dfrac{k_s}{T_s\mathrm{s}+1} \cdot \dfrac{k_n}{T_2^2\mathrm{s}^2 + 2\xi T_2\mathrm{s} + 1}}{1 + \dfrac{57.3\mathrm{g}}{\mathrm{V}}(T_1\mathrm{s}+1)\dfrac{K_i(T_i\mathrm{s}+1)}{\mathrm{s}} \cdot \dfrac{k_s}{T_s\mathrm{s}+1} \cdot \dfrac{k_n}{T_2^2\mathrm{s}^2 + 2\xi T_2\mathrm{s} + 1}}. \tag{13}$$

The closed loop transfer function is obtained with equation

$$H_{u_v}^{n_v}(\mathrm{s}) = \frac{n_v(\mathrm{s})}{u_v(\mathrm{s})} = k_u \cdot \frac{k_v \cdot H_i(\mathrm{s})}{1 + k_k \cdot \dfrac{T_4}{T_3} \cdot \dfrac{T_3\mathrm{s}+1}{\mathrm{T_4s}+1} \cdot k_a \cdot H_i(\mathrm{s})}. \tag{14}$$

In equations (13) and (14) the values of the constants are the ones from equation (9). After calculus, the transfer function in closed loop becomes

$$H_0(\mathrm{s}) = \frac{n_v(\mathrm{s})}{u_v(\mathrm{s})} = \frac{B_2\mathrm{s}^2 + B_1\mathrm{s} + B_0}{A_5\mathrm{s}^5 + A_4\mathrm{s}^4 + A_3\mathrm{s}^3 + A_2\mathrm{s}^2 + A_1\mathrm{s} + A_0}; \tag{15}$$

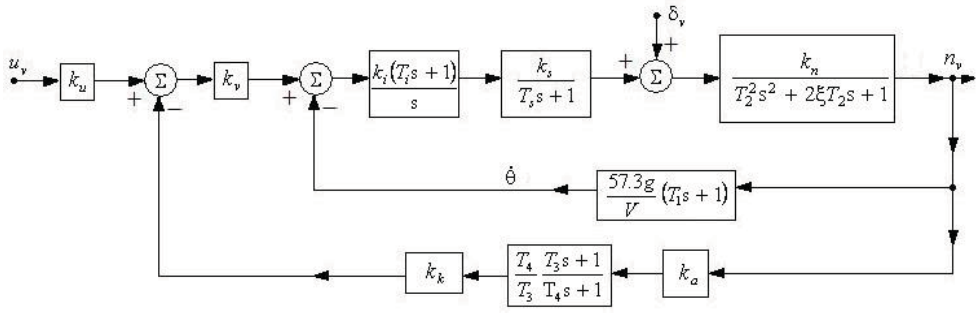

Figure 5: The block diagram of the rockets' angular stabilization system with integrator gyroscope, accelerometer and correction subsystem

the transfer function in open loop is calculated in rapport with the one presented above.

The coefficients that appear in the numerator and dominator of the transfer function (15) are

$$
\begin{aligned}
&B_2 = k_u k_v k_i k_s k_n T_3 T_4 T_i \,;\; B_1 = k_u k_v k_i k_s k_n T_3 \cdot (T_4 + T_i);\\
&B_0 = k_u k_v k_i k_s k_n T_3 \,;\\
&A_5 = T_3 T_4 V T_s T_2^2 \,;\; A_4 = 2\xi T_3 T_s T_4 V + T_3 V T_2^2 (T_3 + T_4);\\
&A_3 = T_3 T_s T_4 V + T_3 V (T_s + T_4) \cdot 2\xi T_2 + T_3 V T_2^2 + \\
&\quad + 57.3 g T_3 T_1 T_4 k_i k_s k_n T_i \,;\\
&A_2 = T_3 V (T_s + T_4) + T_3 V \cdot 2\xi T_2 + 57.3 g T_3 T_1 T_4 k_i k_s k_n T_i + \\
&\quad + k_i k_s k_n T_i \cdot 57.3 g T_3 (T_1 + T_4) + k_k k_a k_i k_s k_n T_4 V T_3 T_i \,;\\
&A_1 = T_3 V + 57.3 g T_3 (T_1 + T_4) k_i k_s k_n + 57.3 g T_3 k_i k_s k_n T_i + \\
&\quad + k_k k_a k_i k_s k_n T_4 V (T_i + T_3);\\
&A_0 = 57.3 g T_3 k_i k_s k_n + k_k k_a k_i k_s k_n T_4 V \,.
\end{aligned}
\tag{16}
$$

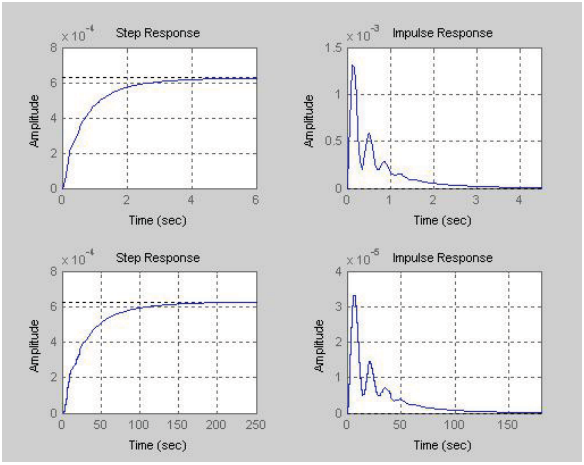

Figure 6: The indicial functions and responses to impulse input in the complex and discrete planes for the system from figure 5

For the above system one obtains, using a Matlab program and a Simulink model, the indicial functions in the complex plane and in discrete plane, responses to impulse input in the complex and discrete planes and time variations of the rocket's overload and of the pitch angular velocity. For the system from figure 5, the indicial functions and responses to impulse input in the complex and discrete planes are presented in figure 6 (the first two graphics correspond to the complex plane, while the last two correspond to the discrete plane).

The program calculates the matrices that describe the state equations of the system in the complex or discrete plane, the poles of the system, the zeros, the transfer functions in complex description or in discrete description, the stability margins and so on.

For the stabilization system one plots the time variation of the system's output – rocket's overload (n_v) and time variation of the pitch angular velocity $(\dot{\theta})$ - figure 7. From these graphic characteristics and from the analysis of the system's eigenvalues (poles) one notices that the system is a stable one with very dynamic properties.

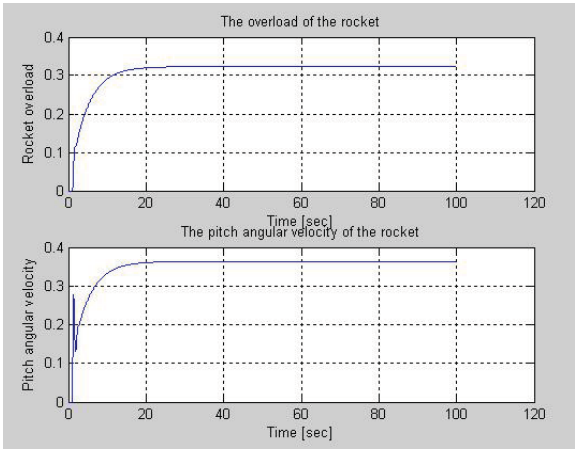

Figure 7: Time variation of the rochet's overload and time variation of the rocket's angular velocity

4. IDENTIFICATION OF THE TWO SYSTEMS USING THE NEURAL NETWORKS' METHOD

Flying parameters' modification and atmospheric disturbances lead to difficulties in stability derivates calculus and to flying objects' models stabilization.

That's why one may use identification methods or state estimate methods [3], [4], [5], [6], [7], [8]. The identification method presented in this paper is based on a neural networks' use. For an off-line identification [3], a feed-forward neural network is used; the network is trained by minimizing the quadratic quality indicator $J(k)=\frac{1}{2}e^2(k), e(k)$ being the training error. The dynamics of the rockets' movement may be described by equation

$$y(k)=f\left(y(k-1)\,y(k-2)\cdots y(k-n_y)\;u(k-q)\cdots u(k-q-n_u+1)\right), \quad (17)$$

with $y=\theta-$ the pitch angle, $u=u_v-$ rocket's command, $q-$ dead time; n_y and n_u express the system's order.

If nothing is known about the control system (n_y, n_u, q, f and n_h- the number of hidden layer neurons), by identification one determines these parameters. So that, starting from minimal neural network's architecture (numbers n_u, n_h, n_y and q) and imposing a value for the error $e(k)$ and a maxim number of training epochs, the neural networks begins the training process. If the error $e(k)$ doesn't tend to the desired value then n_u, n_y and n_h are modified [3].

For identification process's simulation of the rockets' dynamics with neural network one may use the discrete transfer function associated to the system. A neural network with one hidden layer is chosen. This network is characterized by $n_u=1, n_y=3, n_h=5$ and $q=0$. One chooses calculus steps (p), which is equal with vector y's components number (the values at respective moments of the control system). The matrix of neural network P is obtained (it has the dimension $\left((n_u+n_y)\times(p-3)\right)$. Also, matrix T (of desired output of the network, which represents control system's output values matrix) is the matrix of the system outputs' values at time moments corresponding to the calculus steps;

$$\dim(T)=n_e\times(p-3); \quad (18)$$

n_e is the output neurons' number (here $n_e=1$).

After the training process, the two signals (the output of the system from figure 2 - blue color and the output of the NN - red color) overlap (figure 8).

Neural network's training is made using instruction "train" till the moment when

$$e(k)=y(k)-\hat{y}(k)\rightarrow e_{\text{imposed}}(k)=10^{-15} \quad (19)$$

or until the number of training epochs is reached (in our example this number has been chosen 10000). In figure 9 the dependence between error $e(k)$ and training epochs' number is presented.

By neural network's training pseudo – neurons weights matrix W_1 and hidden layer neurons weights vector W_2 are obtained. Also, vectors B_1 and B_2, which contains polarization coefficients' values (bias) for neurons from hidden layer and for output neuron, respectively, are obtained. For this stabilization system they are

$$W_1=\begin{bmatrix} -6.4859 & 5.1131 & 7.2158 & -28.3934 \\ 7.2276 & -3.7265 & 1.8016 & 34.9041 \\ -5.8420 & 10.9790 & -7.7418 & -8.5953 \\ -9.3483 & -1.0506 & 5.3482 & 28.8782 \\ -12.1872 & -2.0662 & 8.4692 & 0.1911 \end{bmatrix}; B_1=\begin{bmatrix} 2.5003 \\ -3.5227 \\ 1.2729 \\ -1.6618 \\ -1.3135 \end{bmatrix}; \quad (20)$$

$$W_2=[0.0925\ -0.2145\ -0.5448\ 0.044\ -0.2575], B_2=[-0.0217].$$

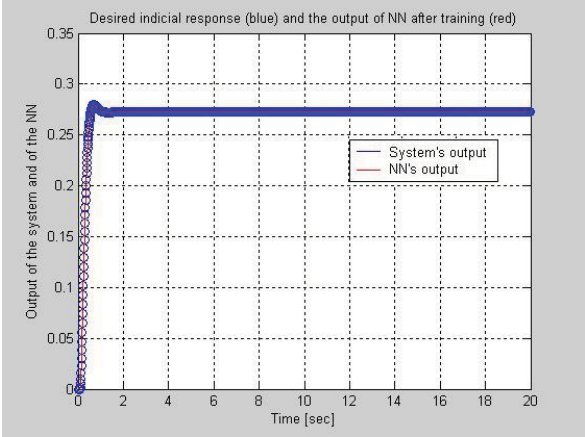

Figure 8: The output of the system from figure 2 (blue color) and NN's output (red color) after training.

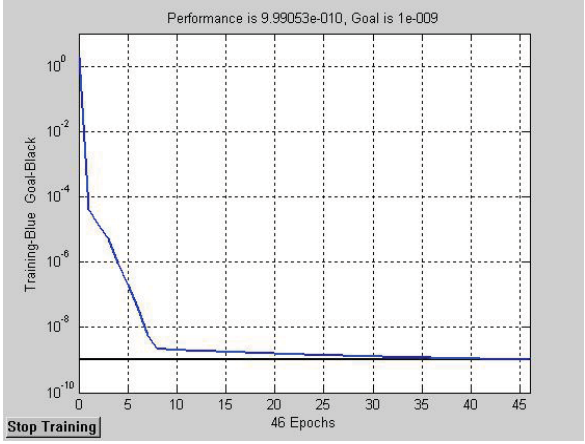

Figure 9: Dependence between the error of the training process and the training epochs' number

Same graphics (figure 10 and figure 11) are obtained for the system with integrator gyroscope from figure 5. These graphics are presented below. The structure of the identification neural network is the same. The weights matrices and the bias vectors are also obtained using the Matlab/Simulink program.

$$W_1 = 10^4 \begin{bmatrix} 5.5484 & 3.2307 & 1.4228 & -0.0007 \\ -3.0391 & -0.4921 & 3.2999 & 0.0031 \\ 0.9250 & -4.1686 & 3.6519 & 0.0023 \\ -0.2282 & 5.2321 & 3.8777 & -0.0009 \\ 4.0518 & -0.5726 & -3.3522 & 0.0026 \end{bmatrix}; B_1 = \begin{bmatrix} -4.9245 \\ -0.5252 \\ -0.7547 \\ -3.3678 \\ 0.6402 \end{bmatrix}; \quad (21)$$

$$W_2 = [0 \ -0.0022 \ 0.0015 \ 0 \ 0.0022], B_2 = [-0.0014].$$

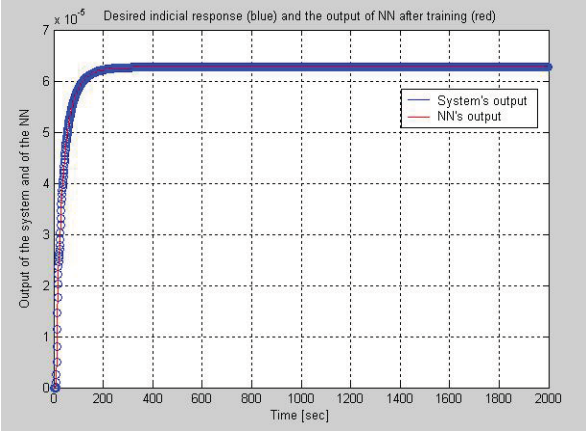

Figure 10: The output of the system from figure 5 (blue color) and NN's output (red color) after training.

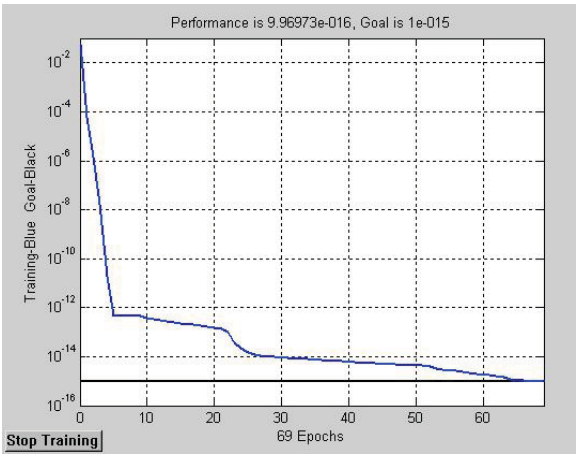

Figure 11: Dependence between the error of the training process and the training epochs' number

5. CONCLUSIONS

The paper presents two angular stabilization systems of the rockets in vertical plane using differentiator or integrator gyroscope. One has determined the transfer functions (in closed loop or in open loop) of the two systems; a study of stability is made. All the eigenvalues of the systems are placed in the left complex semi-plane. This is a proof of systems' stability. The systems respond very fast to a step input – the duration of the transient regimes is about 1.5 seconds in the case of the system from figure 2 and 2.5 seconds in the case of the system from figure 5. That means that the use of a differentiator gyroscope is better than the use of an integrator one. For both systems, one obtains, using a Matlab/Simulink program the indicial functions in the complex plane and in discrete plane, responses to impulse input in the complex and discrete planes. The identification of the two systems is made using neural networks. Using this method, one obtained the indicial responses of the systems and of the neural networks (these signals overlap), the weights and the biases of the neural networks and so on. One also presented the dependence between the error of the training process and the training epochs number for the two systems. The training process lasts longer in the case of the system with integrator gyroscope (69 epochs) compared with the system with differentiator gyroscope (46 epochs). This means that the first system (figure 2) is better (the imposed value of the error and the maximum epochs number is the same for the two systems).

Acknowledgments

This work was supported by the strategic grant POSDRU/89/1.5/S/61968 (2009), co-financed by the European Social Fund within the Sectorial Operational Program Human Resources Development 2007 - 2013.

References

[1] I. Aron, R. Lungu *Automate de stabilizare si dirijare*, Editura Militara, Bucharest, 1991.

[2] C. Teisanu, M. Calbureanu, *Sintering parameters influences on the iron base self-lubricating bearing porosity*, Proceedings of the International Conference on Materials Science and Engineering Bramat 2003, Brasov, Vol. I, pp. 158-163.

[3] M. Donald, *Automatic Flight Control Systems.* New York – London – Sidney – Tokyo – Singapore, 1990.

[4] J. Kaur, S. Singh, K.S. Kahlon, P. Bassi, *Neural Network – A Novel Technique for Software Effort Estimation.* International Journal of Computer Theory and Engineering, Vol. 2, no. 1, 2010.

[5] R. Shukla, A.K. Misra, *Estimating Software Maintenance Effort – A Neural Network Approach.* ISEC'08, February 19-22, 2008, Hyderabad, India.

[6] R. Lungu, *Automatizarea aparatelor de zbor.* Editura Universitaria, Craiova, 2002.

[7] K.S. Narendra, J. Balakrisman, *Adaptation and Learning Using Multiple Models Switching and Tuning.* IEEE Control Systems, 1995.

[8] K. Lau, R. Lopez, E. Onate, *Neural Network for Optimal Control of Aircraft Landing Systems.* World Congress on Engineering 2007, Vol. 2, July 2-4, 2007, London.